Compliance Analysis and Vibration Control of the Safe Arm with MR-based Passive Compliant Joints

Seung-kook Yun*, Seong-Sik Yoon*, Sungchul Kang*,

In-teak Yeo**, Munsang Kim*, and Chong-won Lee*

* Advanced Robotics Research Ce nter, Korea Institute of Science and Technology, Sungbuk-ku, Seoul 136-791, Korea

(Tel : 82-2-958-6743; Fax : 82-2-958-5629; E-mail: arumi@kist.re.kr)

** Intelligent Mechanical System Research Dept., Electro-Mechanical Research Institute, Hyundai Heavy Industries Co., Ltd.,

Mabuk-ri, Kuseong-myun, Yongin-shi, Kyunggi-do 449-716, Korea

(Tel : 82-31-289-5263; Fax : 82-31-289-5150; E-mail: ityeo@hihi.co.kr)

Abstract: In this paper, a design and control of the safe arm with passive compliant joints(PCJ) is presented. Each PCJ has a magneto- rheological damper and maximum 6 springs. Compliance analysis in Cartesian space is performed with the compliance ellipsoid; this analysis shows a map between compliance in the joint space and compliance in Cartesian space. Vibration control of the arm using an input shaping technique is also presented; the results of a simulation and an experiment prove that a fast motion of the safe arm without residual vibration can be performed.

Keywords: Manipulator, Passive Compliant Joint, Magneto-rheological Damper, Compliance Ellipsoid, Input Shaping Technique

1. INTRODUCTION

Robots are recently expected to provide various kinds of service directly to human in human-robot coexisting environment. Considering human-robot interaction, safety is one of the most important issues to be accomplished. To make a compliant robot arm can be a good way to greatly enhance the safety issues. Generally there are two strategies to realize the robot compliance: *active* and *passive*. Active compliance approach usually makes use of the feedback signals from force/torque sensors equipped either on a robot hand or at a joint of links so that the robot controller may detect the applied external force and generate a proper response. The active compliance approach generally has a limit in delayed control and incomplete safety in case of electrical malfunctioning, even though it can offer a high programming ability for compliance control. In this case, manipulators with active compliance function may cause either damage to human or failure of power transmission due to the shock when unexpected contact occurs. On the other hand, passive compliance can be realized by applying a passive mechanism to produce an appropriate reaction to the applied forces.

There have been several attempts for passive compliance mechanism. Laurin-Kovitz[1] made a programmable passive impedance(PPI) component with an antagonistic nonlinear spring and a binary damper. Morita and Sugano[2] proposed a Mechanical impedance adjuster (MIA) with a variable spring and a pseudo-damper implemented by an electromagnetic brake. Okada[3] used Programmable passive compliance (PPC) shoulder mechanism with a variable-stiffness spring. Yamada[4] made a passive visco-elastic covering. Lim and Tanie[5] proposed a passive joint with a linear spring and a linear damper between a mobile part and an arm .

As shown in the previous work, there are approaches which do not use a covering and cannot attenuate an impact force on unexpected collisions; vibration may occur due to the absence of dampers; implementation is very difficult due to the complexity of the joints. Thus, in this work, a safe arm design overcoming these disadvantages is proposed.

In this paper, the design of the safe arm with a magneto-rheological rotary damper and rotary springs is introduced. MR fluid is a suspension including micro-sized, magnetizable particles in carrier fluid. Yield stress of the fluid can be controlled precisely by altering strength of applied magnetic field[6]. The MR fluid has broad operational temperature range, fast response time, and highly dynamic yield stress. An MR damper using the MR fluid has the following advantages. At first, it consumes less power and has less hysteresis than an electromagnetic damper. Also it enable smoother and quieter operation than an electromagnetic damper. Secondly, variable damping control is possible. A rotary MR damper with viscous damping property can be implemented by controlling applied current. Finally, through simple and modular design, power ratios versus weight and size can be greatly increased. With this MR damper and rotary springs, a passive compliance joint(PCJ) is developed for the safe arm of a service robot.

Since the PCJ has compliance, we need to analyses the compliance of the manipulator in Cartesian coordinate. Compliance ellipsoid for the safe arm is visualized and used for the analysis in terms of compliance mapping between Cartesian space and the joint space. With this ellipsoid, we can evaluate the compliance at any point where the collision occurs. We can also see which configuration of the arm has more compliance at a specified point.

When controlling the manipulator with PCJs, unwanted vibration has occurred because of springs included in each PCJ. Passive compliance meets the safe criteria but causes vibration during the movement of the arm. Although the damper of a PCJ may suppresses some portion of the vibration, a fast motion cannot be performed without vibration. This vibration may cause an unstable control or unwanted collision to the environment in view of the safety. To reduce the vibration, input shaping technique(IST)[7] is introduced. In suppressing unnecessary vibrations, the capability of IST has been proved through various applications.

In this work, a proper design of a controller with IST filter for the manipulator with PCJs is conducted. A few simulations and experiments using the proposed controller are performed.

This paper is organized as the following order. Section 2 introduces the design of the PCJ and the manipulator. Section 3 describes the compliance analysis in Cartesian coordinates and joint coordinates based on a compliance ellipsoid. Section 4 features the controller design with an IST filter for the manipulator with PCJs and some simulation and experiment results are shown. In Section5, a conclusion and further works are stated.

2. SAFE ARM DESIGN

2.1 Design of passive compliant joint(PCJ)

The design of the passive compliant joint [8] is shown in Fig. 1. The PCJ is composed of a magneto-rheological (MR) rotary damper and rotary springs. The rotary springs become a source of vibration while they give a PCJ's compliant property. Therefore a viscous damper is implemented using the developed MR damper. The PCJ has a resolver sensor of 16-bits high resolution to read the relative position between the reducer(harmonic drive) and the link due to the spring displacement. The relative position is converted into a relative velocity signal through numerical differentiation and sent to a damping tuner which converts coulomb friction property of the MR damper into viscous one. Note that the damper and spring are located in parallel between the reducer and link. A driving unit is made up of a DC motor, an encoder, a timing belt, and a harmonic drive gear.
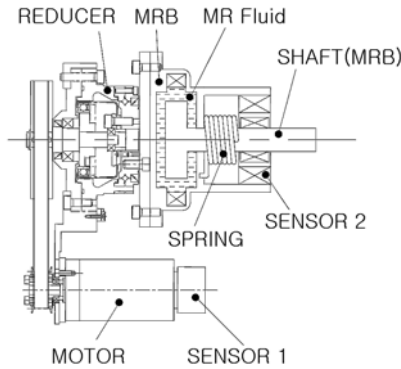

Fig. 1 Design of the passive compliant joint mechanism

In the MR damper, MRF-132LD manufactured by the Lord Corporation[9] is used. Each damper of a PCJ has its own parameter value. Experimental test with this three MR dampers shows that there is almost linear relation between applied current and generated torque by MR damper in [8].

The next component of the PCJ is rotary springs. Fig. 2 shows a three-dimensional model of the spring component. The upper part and lower part are assembled and rotate relatively. The torsional stiffness of the spring component is calculated as follows:

$K = n_K k \quad (Nm/rad)$,

Where k is the spring constant of each linear spring and n_K is the number of springs. The joint stiffness depends on the number of springs. The implemented parameters are summarized in [8].
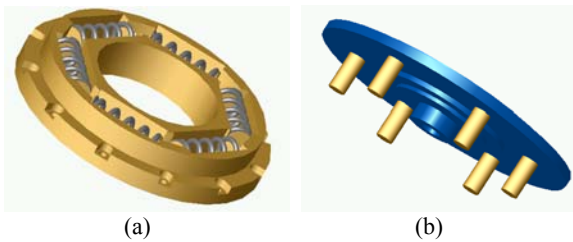

Fig. 2. A three-dimensional model of the spring component:
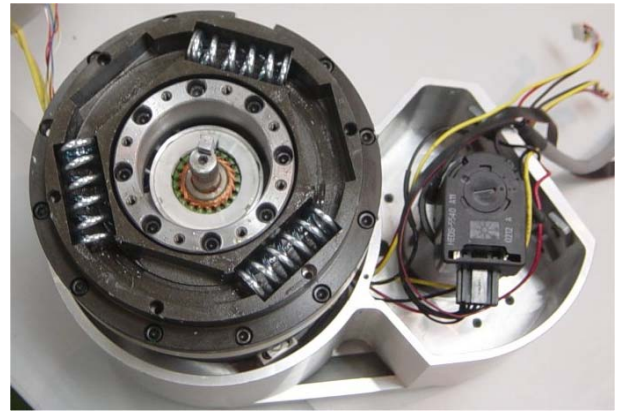(a) a lower part, (b) a upper part.

Fig. 3. A complete set of the PCJ

The springs and damper are assembled as Fig. 1 where a cross roller bearing is inserted between the springs and damper. Note that the two components build a parallel structure with a housing. Finally, a passive compliant joint with a housing, a motor, pulleys, a harmonic drive reducer, and a link is shown in Fig.3

2.2 Visco-elastic Cover Design

In this subsection a visco-elastic cover to attenuate a collision force is addressed. The covering can be modeled simply by a spring and a damper as shown in Fig.4. If a robot arm is represented by a simple body with a mass M_e, the collision model is obtained as follows when the arm collides with a human:

$$M_e \ddot{\varepsilon} = F_{human} ,\qquad(1)$$

where

$$F_{human} = -B_u \dot{\varepsilon} - K_u \varepsilon ,\qquad(2)$$

$$B_u = \frac{A_c \eta_c}{Z_c}, K_u = \frac{A_c G_c}{Z_c} ,\qquad(3)$$

M_e is a mass, F_{human} is a force acting on a human, ε is the compressed displacement of the cover, A_c is the contact area of the cover, η_c, G_c, Z_c are the viscous coefficient, elastic modulus, and thickness of the cover each. The units of η_c, G_c, Z_c are [Pa], [Pas], and [m], respectively.
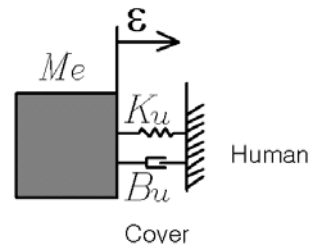

Fig. 4. A diagram for modeling a visco-elastic cover.

Three types of a urethane foam including EGR-2, HR-80, and SR-S-24 are compared to each another. The detail SPECs of each urethane foam are shown in Table.1. The thickness of the cover is set to 5 [mm] taking account of the size of the arm. A simulation on the effect of the visco-elastic covers is performed to select an appropriate visco-elastic cover. The parameters used in the simulation is as follows:

$M_e = 10.7 kg$, $V_c = 0.125 m/sec$, $A_c = 1520 mm^2$,

where V_c is velocity of the effective mass when the impact occurs. Each parameter is selected considering the condition of the safe arm when opening the door [4].

Table.1. SPEC of the urethane foams

Urethane Foam	Z_c [mm]	η_c[Pa]	G_c[Pas]
EGR-2	5.0	520	2794
HR-80	5.0	804	3260
SR-S-24	5.0	1210	48000

Table.2. absorbed impact force and mean force to human

Urethane Foam	Absorbed force [N.sec](%)	Mean Force
EGR-2	0.65 (49%)	16
HR-80	0.86 (64%)	21
SR-S-24	1.5 (111%)	38

Absorbed impact forces and mean forces to human are shown in Table.2. Considering these factors and the process ability, PORON SR-S-24 is finally selected. A simulation result using the SR-S-24 is shown in Fig.5.
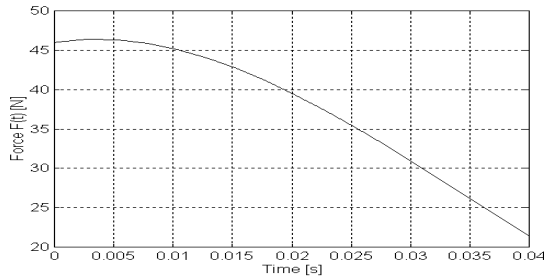

Fig.5. SR-S-24 property at impact force

2.3 Safe Arm Design

A safe arm with MR-based passive compliant joints and a visco-elastic cover is designed for service robot applications. A 6-dof safe arm whose payload is 3 (Kg) has been developed as shown in Fig.6.

Fig. 6. PSR-2 with the safe arm.

This arm is used for the PSR-2 (Public Service Robot)

developed at the KIST (Korea Institute of Science and Technology). As the first step for the implementations, PCJs are equipped into three joints in the service robot arm.

3. COMPLIANCE ANALYSIS

3.1 Definition of the Compliance Ellipsoid

The developed PCJ has a feature of the manipulator programmable compliance via springs and a MR damper. This compliance basically works in the joint space since the PCJ is joint-based mechanism. When we want to analyses the compliance of the safe arm in the Cartesian coordinate, a compliance ellipsoid[3] would be useful.

The compliance ellipsoid sets forth the displacement of the end effector in all direction of the unit vector force. The volume of compliance ellipsoid can be a useful parameter to check quantity of compliance. Especially for the safe arm, lager volume of the compliance ellipsoid guarantees more safety. When the safe arm comes to collide something, the compliance ellipsoid volume of the collision point can tell the safety of the point.

When there is a force F to the end effector, a joint torque of each joint is as follows:

$$\tau = J^T f , \qquad (4)$$

where J is a jacobian matrix of the manipulator.

With the relation between a force and a displacement of the end effector:

$$f = K \Delta x \qquad (5)$$

where K is a spring constant matrix in Cartesian coordinate, and Δx is a displacement of the end effector.

the relation between a joint torque and a displacement of a joint angle is:

$$\tau = K_q \Delta \theta \qquad (6)$$

where K_q is a spring constant matrix in the joint coordinate,

$$K_q = \begin{bmatrix} K_1 & 0 & 0 \\ 0 & K_2 & 0 \\ 0 & 0 & K_3 \end{bmatrix} \qquad (7)$$

for the 6-DOF safe arm with 3 PCJs. The K_1, K_2, and K_3 are spring constants of each PCJ.

From equations (4)-(7), the compliance matrix in the cartesian coordinate is obtained as follows:

$$C = K^{-1} = J K_q^{-1} J^T \qquad (8)$$

Using the singular value decomposition, the C can be rewritten

$$C = USV^T$$
$$= [U_1 \ U_2 \ U_3][s_1 \ s_2 \ s_3]V^T . \qquad (9)$$

The compliance ellipsoid is defined in three dimensional space whose axis are $s_i U_i$ *(i=1,2,3)*. Since each column vectors of the matrix U is a unit vector, the volume of the compliance ellipsoid is as follows:

$$v = s_1 s_2 s_3 \qquad (10)$$

Finally, the volume of the compliance ellipsoid corresponds to the multiplication of all eigenvectors of the compliance matrix.

3.2 Compliance ellipsoid of the safe arm

Fig.7 shows a few compliance ellipsoid according to a few configurations of the safe arm. All drawings are 2D-plotted, and 100N force is used in equations instead of the unit force

because the first joint of the arm is along the axis of the base, and a unit force is too small to visualize. As expected, the safe arm has only 2-dimensional or even 1-dimensional compliance at singular position. In this case, the compliance ellipsoid has zero volume as shown in Fig. 7(d)
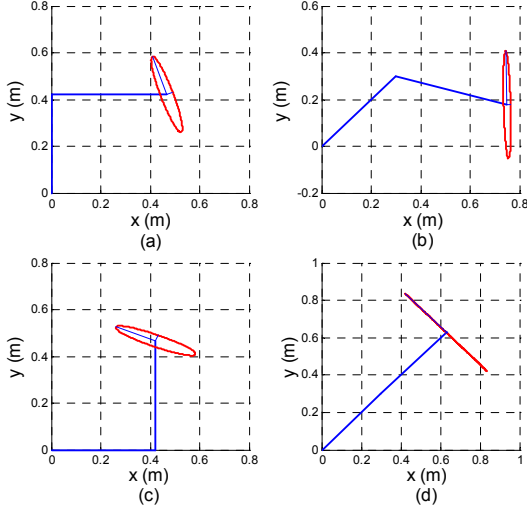

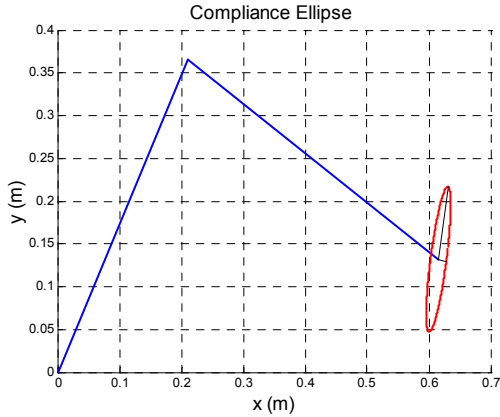Fig.7 Compliance ellipsoid with 100N force

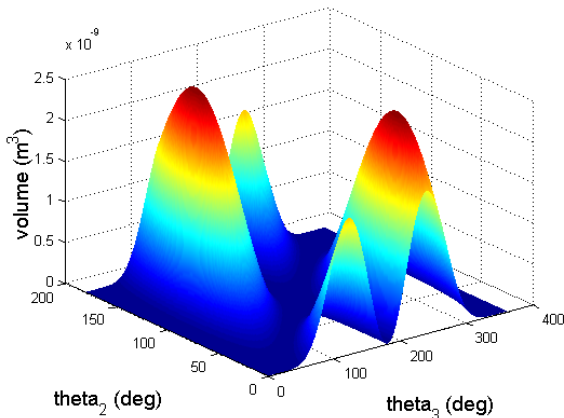Fig.8. Arm configuration with maximum compliance

Fig.9. Compliance map with joint angles

Fig.8 shows the configuration of the safe arm which produces the maximum compliance, i.e. the maximum volume of the compliance ellipsoid within workspace of the arm.

Using these data of the volume, we can make a map which represents quantity of compliance depending on the configuration of the safe arm. With this map in Fig.9, we can find which configuration give more compliance or not with easy. Also this map can be used in the control strategy; path planning can be designed by using this compliance map.

4. CONTROLLER DESIGN

4.1 Position control

In [8], a model of one-DOF arm with a PCJ is introduced and its controllability is analyzed. The result shows that a determinant of the controllability matrix is not zero as long as K is not zero, therefore the system with a PCJ is always controllable regardless of the viscous damping coefficient.

A conventional PID controller is used for a joint control:

$$\tau_m^i = -K_P^i(\theta_m^i - \theta_d^i) - K_D^i(\dot{\theta}_m^i - \dot{\theta}_d^i) - K_I^i \int_{t_0}^{t} (\theta_m^i - \theta_d^i)d\tau \quad (11)$$

where θ_d^i is a constant desired angle for the i-th joint, τ_m^i is a motor torque considering reduction ratios, and θ_m^i is a angle of each motor. To compensate for position error due to the gravity in steady state, the following control method similar to that of the passive joint called the MIA [3] is used:

$$\tau_m^i = -K_P^i(\theta_m^i - \overline{\theta}_d^i) - K_D^i(\dot{\theta}_m^i - \dot{\overline{\theta}}_d^i) - K_I^i \int_{t_0}^{t} (\theta_m^i - \overline{\theta}_d^i)d\tau , (12)$$

where

$$\overline{\theta}_d^i = \theta_d^i + G^i(\theta_d^1, \cdots, \theta_d^6)/K^i , \quad i = 1,2,3 \quad (13)$$

G^i means the i-th term related to gravity in the arm dynamics and K^i represents a spring constant for the i-th axis. This control method has an advantage that there is no loss of the passive compliance property during position control because the spring and damper can be passively operated

4.2 Vibration reduction

Although the PCJ enables passive compliance for the safe arm, it also can be a source of unwanted vibration. This vibration may cause an unstable controller or unwanted collision to the environment in a view of the safety. Especially, a lot of residual vibration can be occurred after a fast motion of a PCJ.
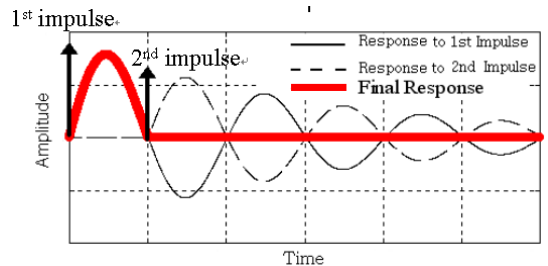

Fig.10.vibration suppression via IST

As an effective solution to reduce this vibration, input shaping technique(IST) based on an impulse response is proposed. The IST uses two impulses to get rid of residual vibration. Fig.10 shows how the IST works with two impulse

responses. The IST can be considered as a simple filter since these two impulses are to be convoluted with a desired trajectory or an open loop control input.

The IST can be an excellent solution to reduce vibration for a linear time invariant system, but it is not much effective for a non-linear or a time varying system. Since the safe arm is a time varying system in which a moment of inertia is changed during the rotation of the next joint, a time varying IST is needed.

A thesis that a proper IST filter with two impulses can eliminate a residual vibration of a time invariant system is proved by Park[11]. However It is almost impossible to identify magnitudes of impulses and a time for the second impulse. There have been a couple of studies to apply the IST to a time varying system. Rappole[12] applied a time varying input shaping technique(TVIST) to a two link flexible manipulator, Park[13] proposed a practical method of TVIST to reduce vibration of an industrial robot. The former used a look-up table which contained the information of configuration dependent frequency, and the latter used a simple equation relating a period of vibration and a length from the swing axis to the wrist axis along the horizontal line. Although these two methods can be a practical method to reduce vibration of a time varying system, an estimation of the second impulse time is always incorrect because of dynamics of the system.

In this work, we used a modified TVIST considering the dynamics of the safe arm. The most important point on the TVIST is an exact guessing of the second impulse time. In the previous TVISTs, a guessing is implemented from experimentally or theoretically gathered data. The guessed time, however, is always faster or later than the exact time. As for the safe arm, the guessed time is faster when a inertia is increasing, later when decreasing because of dynamics of the system. So, we use the practical method by choosing the mean value of the guessed time in TVIST and the second impulse time which is calculated at the time of the first impulse.

4.3 Simulation results

In this section, a simulation have been performed to prove that the proposed method is valid for a practical use. Simulations for the IST on the 3rd axis(LTI)   and the modified TVIST on the 2nd axis(TV) are implemented each.
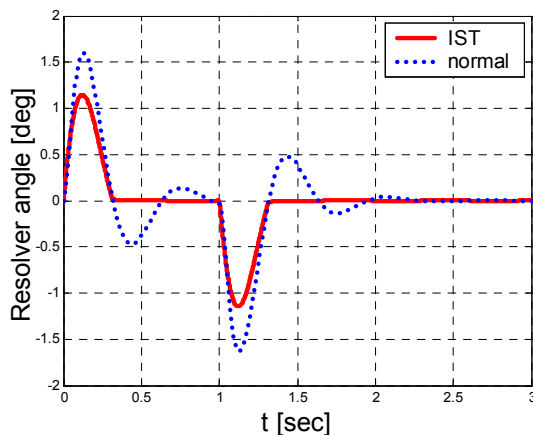

Fig.11. Simulation: resolver angle of 3rd joint

The 3rd joint of the safe arm is nearly a time invariant system, so we can use the conventional IST for 3rd Axis.

Fig.11 show the simulation result of 3rd joint when the IST is implemented. Desired path is 60 degree per a second, a resolver angle between motor angle and 3rd link angle is shown for the magnitude of vibration. Since the 3rd joint is considered as a LTI system, the perfect elimination of residual vibration is possible.

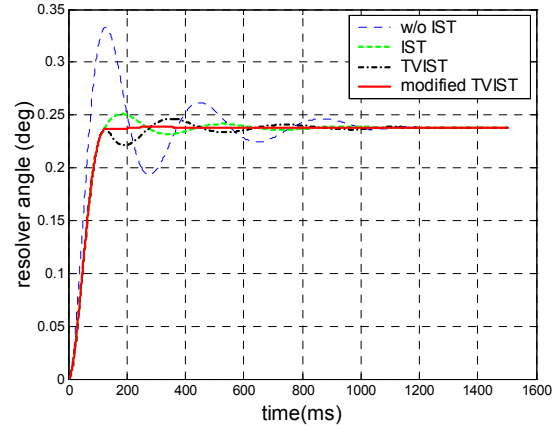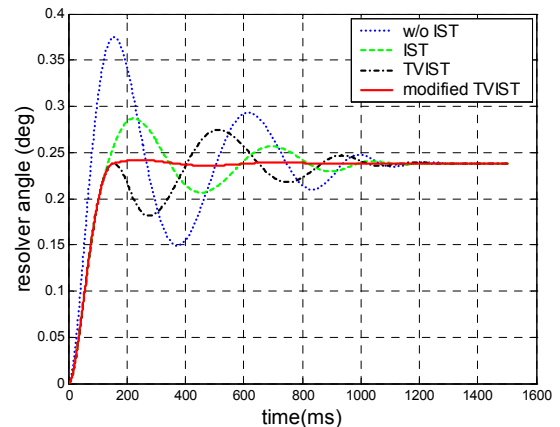Fig.12. Simulation: inertia changes linearly

Fig.13. Simulation: inertia changes with a sinusoidal form

In Fig.12 and Fig.13, simulation results on 2nd joint with varying inertia are shown. Inertia is varying as follows:
In Fig.12,

$$J = J_o + 2t \qquad \qquad for \ t < 1$$
$$J = 2 + J_o \qquad \qquad otherwise \qquad (16)$$

In Fig.13,

$$J = J_o + 2\sin(\pi t) \qquad for \ t < 1$$
$$J = J_o \qquad \qquad otherwise \qquad (17)$$

where J_o=0.55 kgm^2, which is the minimum theoretical value of the 2nd axis inertia. Open loop control with a step response is performed so that an effect of a proposed TVIST can be clearly shown.

In both cases, modified TVIST reduces most of vibration. TVIST gives a bit better result compared to the conventional IST.

4.4 Experimental results

An experiment of 3rd joint of the safe arm is presented. UMAC motion controller is used for controlling the six-dof safe arm, and MR dampers are independently controlled by a separated controller. Each encoder signal is sent to PC via USB and RS-232C port. A desired trajectory is 60 deg/sec which is the same as one of the previous simulation.

Fig.14 and Fig.15 show the result of the experiment. With a step velocity command, the IST reduces residual vibration of 3rd axis dramatically. The difference between the angle of a starting point and steady state is from gravity. As shown in Fig.14, IST works well even in gravity.
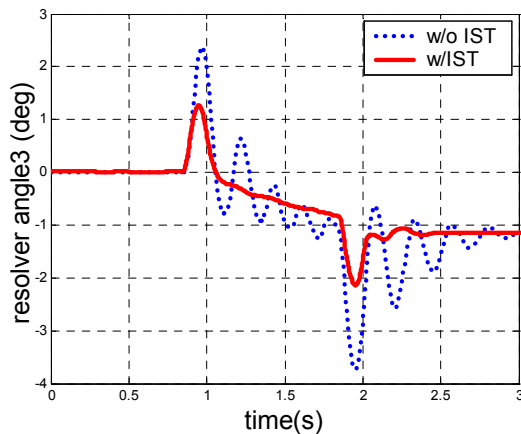

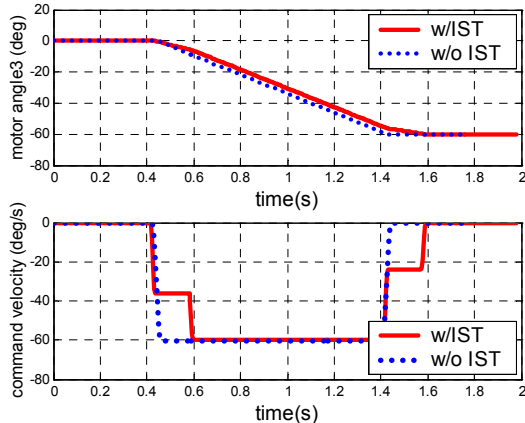Fig.14. Experiment: resolver angle of 3rd joint

Fig.15. Experiment: motor angle and command velocity

5. CONCLUSION

The new safe arm for a service robot with passive compliant joints via springs and a MR damper and a covering is designed. Compliance analysis of the arm in the Cartesian coordinate is performed through the compliance ellipsoid. A proper controller considering reduction of residual vibration by IST and TVIST is proposed for the safe arm. The simulation results and experimental result shows that IST can work properly on the safe arm.

As a future research, an experiment of TVIST on the 2nd and 1st axis can be performed. Control of the link angle θ_L also has to be performed for the free-motion movement.

REFERENCES

[1] K. F. Laurin-Kovitz, J. E. Colgate, and S. D. R. Carnes, "Design of components for programmable passive impedance," *Proc. of the IEEE International Conference on Robotics and Automation*, pp. 1476-1481, 1991.

[2] T. Morita and S. Sugano, "Development of one-D.O.F. robot arm equipped with mechanical impedance adjuster," *Proc. of the IEEE/RSJ International Conference on Intelligent Robots and Systems*, pp. 407-412, 1995.

[3] M. Okada, Y. Nakamura, and S. Ban, "Design of Programmable Passive Compliance Shoulder Mechanism," *Proc. Of the IEEE International Conference on Robotics and Automation*, pp. 348-353, 2001.

[4] Y. Yamada, K. Suita, K. Imai, H. Ikeda, and N. Sugimoto, "Human-robot contact in the safeguarding space," *IEEE/ASME Transactions on Mechatronics*, vol. 2., no. 4, pp.230-236, 1997.

[5] H.-O. Lim and K. Tanie, "Human safety mechanisms of human-friendly robots: passive viscoelastic trunk and passively movable base," *International Journal of Robotics Research*, vol. 19, no. 4, pp. 307-335, 2000.

[6] J. D. Carlson, D. M. Catanzarite and K. A. St. Clair, "Commercial magneto-rheological fluid devices," *Proc. of Electro-Rheological, Magneto-Rheological Suspensions and Associated Technology*, W. Bullough, Ed., World Scientific, Singapore, pp. 20-28, 1996. (http://www.mrfluid.com/tech_library/mr_fluid.htm)

[7] N.C. Singer, and W.P. Seering, "Preshaping Command Inputs to Reduce System Vibration," *ASME Journal of Dynamic Systems, Measurement and Control*, Vol.112, pp. 76-82, 1990.

[8] S.-S. Yoon, S. Kang, S.-J. Kim, Y.-H. Kim, H.-S. Yim, and M. Kim, " Design and control of a passive compliant joint for human-friendly service robots," *International Conference on Control, Automation and Systems*, CD-ROM, 2002. (http://www.icase.or.kr/)

[9] The LORD Corporation, "Magnetorheological fluid MRF-132LD", *Product Bulletin*, 1999. (http://www.mrfluid.com)

[10] M. Kim, S.-S. Yoon, S. Kang, S.-J. Kim, Y.-H. Kim, H.-S. Yim, C.-D. Lee, I.-T. Yeo, "Safe arm design for service robot," *In Proceedings of The Second IARP -IEEE/RAS Joint Workshop on Technical Challenge for Dependable Robots in Human Environments*, pp. 88-95, Toulouse, France, 2002.

[11] J. Park, P.H. Chang, and E. Lee, "Can a Time Invariant Input Shaping Technique Eliminate Residual Vibrations of LTV Systems," *Proc. of the American Control Conference*, pp. 2292-2297, 2002.

[12] B.W. Rappole, "Minimizing Residual Vibrations in Flexible Systems," *Master thesis, Department of Mechanical Engineering, MIT*, 1992.

[13] H.Y. Park, P.H. Chang, and J.S. Hur, "Time-Varying Input Shaping Technique Applied to Vibration Reduction of An Industrial Robot", *Proc. of the IEEE/RSJ International Conference on Intelligent Robots and Systems*, pp.285-290, 1999.